

# A 1.5GS/s 8b Pipelined-SAR ADC with Output Level Shifting Settling Technique in 14nm CMOS

Yuanming Zhu, Shengchang Cai, Shiva Kiran, Yang-Hang Fan, Po-Hsuan Chang, Sebastian Hoyos, and Samuel Palermo

Analog and Mixed-Signal Center

Department of Electrical and Computer Engineering, Texas A&M University  
College Station, TX, USA

Email: {zymk1989, spalermo}@tamu.edu

**Abstract**—A single channel 1.5GS/s 8-bit pipelined-SAR ADC utilizes a novel output level shifting (OLS) settling technique to reduce the power and enable low-voltage operation of the dynamic residue amplifier. The ADC consists of a 4-bit first stage and a 5-bit second stage, with 1-bit redundancy to relax the offset, gain, and settling requirements of the first stage. Employing the OLS technique allows for an inter-stage gain of  $\sim 4$  from the dynamic residue amplifier with a settling time that is only 28% of a conventional CML amplifier. The ADC’s conversion speed is further improved with the use of parallel comparators in the two asynchronous stages. Fabricated in a 14nm FinFET technology, the ADC occupies 0.0013mm<sup>2</sup> core area and operates with a 0.8V supply. 6.6-bit ENOB is achieved at Nyquist while consuming 2.4mW, resulting in an FOM of 16.7fJ/conv.-step.

**Keywords**—Analog-to-digital converter (ADC), output level shifting (OLS), pipelined-SAR.

## I. INTRODUCTION

As wireline communication data rates climb about 100Gb/s, there is an increased number of receiver front-ends utilizing high-speed analog-to-digital converters (ADCs) that allow for subsequent powerful digital equalization and symbol detection techniques [1]. These converters employ a large amount of time-interleaved unit-ADC channels to achieve the required high effective sampling rates. Sampling in these ADCs is typically performed in several ranks with multiple clock phases per rank and generating these clocks with the required accuracy and jitter performance is a major challenge. Another major issue is maintaining the required signal bandwidth as the interleaving factor is increased. This motivates the development of high-speed low-power unit ADCs that can reduce the interleaving factor for a given effective sampling rate, resulting in smaller area and an overall simpler design.

Successive-approximation-register (SAR) ADC architectures are popular due to their low comparator count and simple digital logic content, making them suitable for compact and power-efficient mid-resolution time-interleaved ADCs [2]. However, the conversion speed is limited in the most common implementation of the successive approximation algorithm that performs sequential single-bit conversion cycles. As shown in Fig. 1, introducing pipelining in the SAR ADC provides improved speed by decreasing the number of conversion cycles per input sampling event. A critical block in this architecture is the amplifier that transfers the residue signal between the two

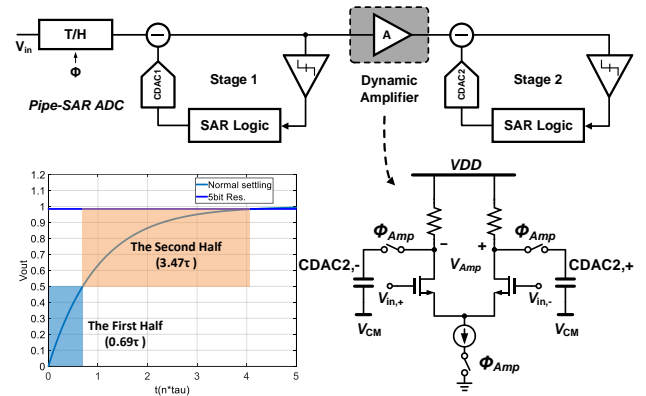


Fig. 1. Pipeline SAR ADC with a dynamic residue amplifier.

pipeline stages. In high-speed converters, conventional opamp-based amplifiers are not suitable due to the excessive static power required to meet settling time requirements. An alternative approach is to use a dynamic residue amplifier that is only activated once over the entire conversion process [3] [8].

While dynamic residue amplifiers have the potential to save power, these topologies require a small  $\tau$  to achieve fast settling times. Satisfying this and maintaining a given gain can result in large dynamic tail current values and increased input transistors that load the first pipeline stage capacitive digital-to-analog converter (CDAC). Given that the smallest CDAC that satisfies the  $kT/C$  noise requirement is desired to reduce input buffer power, this loading can cause significant reference attenuation that must be compensated with an increased range reference buffer that is difficult to implement with low supply voltages. Another issue is kickback noise due to the coupling through the large dynamic amplifier input transistors.

This work presents a single channel 1.5GS/s 8-bit pipelined-SAR ADC that utilizes a novel output level shifting (OLS) settling technique to enable low-voltage operation of the dynamic residue amplifier with low hardware overhead. A detailed discussion of the proposed OLS settling technique that allows for an inter-stage gain of  $\sim 4$  with a settling time that is only 28% of a conventional CML amplifier is given in Section II. Section III provides an overview of the asynchronous ADC architecture and key circuit details. Measurement results from a 14nm CMOS FinFET prototype are presented in Section IV. Finally, Section V provides the conclusion.



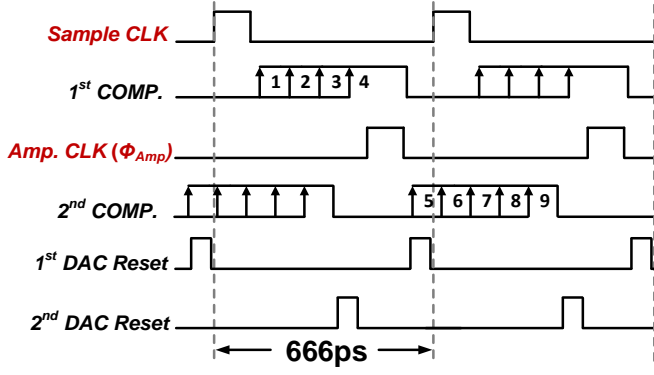


Fig. 4. ADC timing diagram.

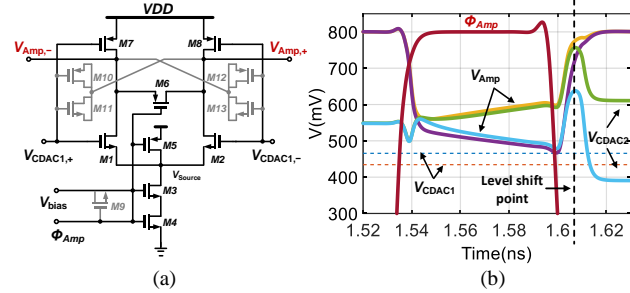


Fig. 5. Inverter-based dynamic amplifier. (a) Schematic and (b) Simulation results.

One potential issue with the proposed amplifier is matching the duration of  $\Phi_{Amp}$  with the 50% settling point. However, high precision is not necessary, as any inaccuracy simply results in a modified gain value that is easily compensated with adjustment of the second stage reference voltages. The jitter specifications on the  $\Phi_{Amp}$  signal are also not prohibitive, as a relatively large 8ps<sub>pp</sub> jitter can be tolerated to achieve 5-bit accuracy at 1.5GS/s.

### III. ADC ARCHITECTURE AND BUILDING BLOCKS

Fig. 3 shows the 8-bit pipelined-SAR ADC with the first pipeline stage converting 4-bits and the second stage converting 5-bits. This 1-bit redundancy between the two stages relaxes the gain, offset, and reference settling requirements of the first stage. The input signal is sampled with a boot-strapped switch that reduces the input sampling time constant and improves high-frequency linearity.  $kT/C$  noise requirements are satisfied with CDAC1 and CDAC2 set at 32fF and 16fF, respectively. Both stages employ parallel comparators that are asynchronously activated sequentially for each conversion step, eliminating the comparator reset delay and offering significant speed-up.

The ADC timing diagram is shown in Fig. 4. After input sampling, the first stage converts 4 bits and holds the residue voltage for partial amplification when  $\Phi_{Amp}$  goes high.  $\Phi_{Amp}$  then transitions low and the level-shifted gain is achieved when the  $\Phi_{OLS}$  pulse is activated with minor modifications in the second stage reference switch logic. The second stage then converts the final 5 bits. Both stage CDACs are reset after their conversions are complete to avoid memory effect, with these reset signals internally generated by the comparator ready signal and input clocks. Independent flipped-voltage followers serve as buffers for the two sets of CDAC reference voltages that are locally decoupled with MOS capacitors. As previously mentioned in Section II, the second-stage reference voltage values are tuned

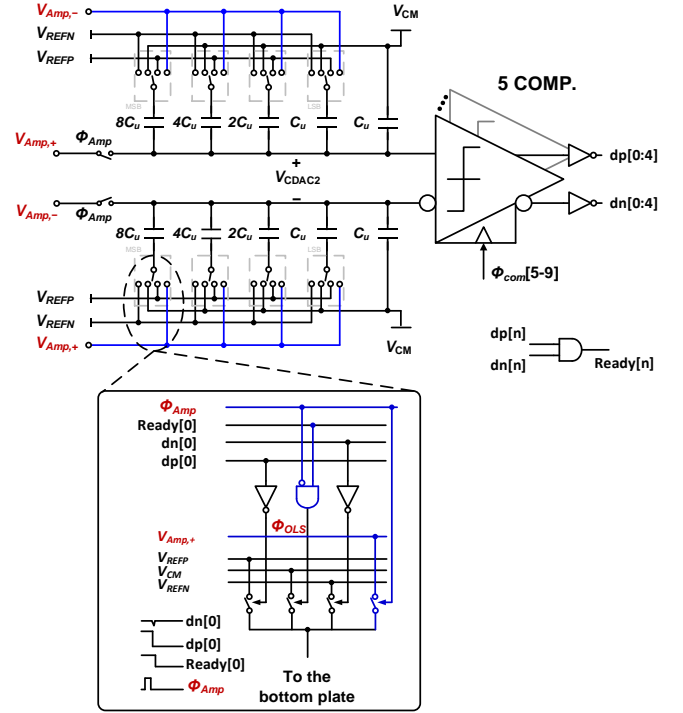


Fig. 6. Second stage reference switch control with embedded OLS technique.

to accommodate any static deviations in the dynamic amplifier gain due to the exact  $\Phi_{Amp}$  pulse width.

#### A. Dynamic Amplifier and Comparators

A clocked inverter-based buffer that achieves a gain of  $\sim 4$  serves as the residue amplifier stage, shown in detail in Fig. 5(a). In addition to the main transconductance transistors M1/2 and M7/8, M3 acts as a current source that is switched on by M4 when  $\Phi_{Amp}$  is activated. The gray transistors improve the dynamic performance, with M10-13 compensating kickback noise and M9 boosting the amplifier startup. When the amplifier is disabled transistors M5 and M6 reset  $V_{Source}$  to VDD and short the differential output, respectively. As shown in the Fig. 5(b) simulation results, resetting CDAC2 allows the amplifier output to start separating from the common mode and then experience an effective doubling after the level shifting.

Dynamic two-stage comparators are used to allow for low-voltage operation in the two pipeline stages. These comparators are foreground offset-calibrated with current-mode DACs.

#### B. Second Stage Reference Switch with Embedded OLS

Fig. 6 illustrates how the OLS technique is included with minor logic changes in the reference switch control to allow both the CDAC2 bottom and top plate to connect to the amplifier output during the amplification phase. As shown in detail for the negative DAC MSB switches, there is an extra right-most switch that connects the bottom plate to the positive input signal when  $\Phi_{Amp}$  is high. An AND gate then produces the  $\Phi_{OLS}$  signal to switch the bottom plate to the common mode when  $\Phi_{Amp}$  goes low and the comparators' ready signals are enabled. Since the extra switch is added to the CDAC bottom plate, there are no speed penalty or reference attenuation issues.

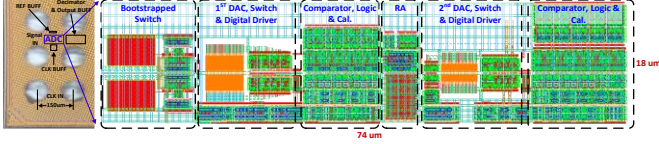


Fig. 7. Prototype ADC chip micrograph.

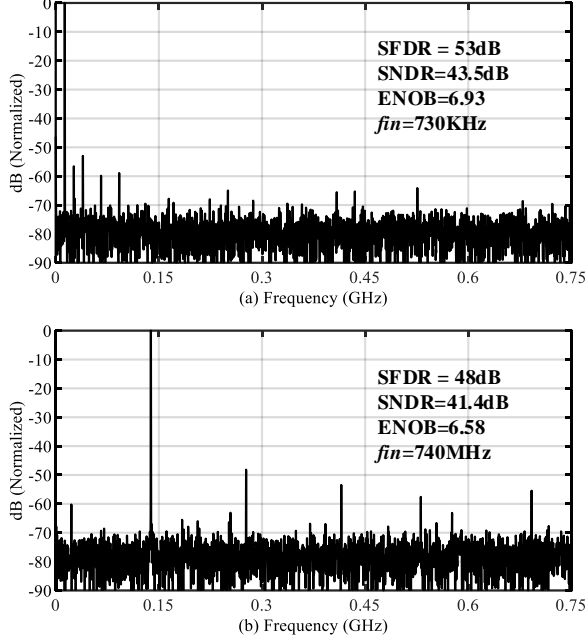


Fig. 8. 1.5GS/s ADC normalized output spectrum for (a) low frequency input and (b) close to Nyquist input. (Decimated by 18, 4096 FFT point).

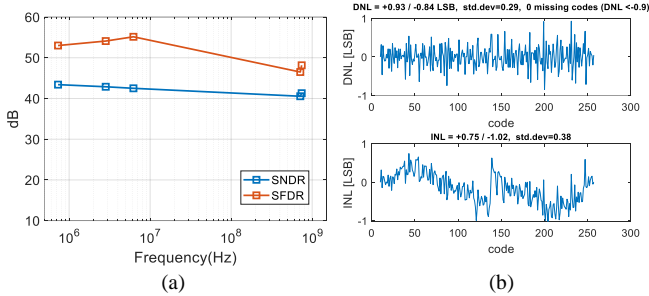


Fig. 9. (a) SNDR and SFDR vs. input frequency. (b) DNL and INL plots.

#### IV. EXPERIMENTAL RESULTS

Fig. 7 shows the chip micrograph of the pipelined-SAR ADC, which was fabricated in a 14nm CMOS FinFET process and occupies an active area of 0.0013mm<sup>2</sup>. The ADC is powered from a 0.8V supply and has a 460mV<sub>pp,diff</sub> full-scale input range with a common mode of 500mV. Testing is performed with an initial foreground offset calibration for all comparators. Fig. 8 shows DFTs of the ADC output when operating at 1.5GS/s. The achieved SNDR is 43.5dB and 41.4dB for low frequency and close to Nyquist inputs, respectively, translating to 6.93 and 6.58 bits ENOB. Fig. 9 shows that the ADC maintains over 40dB SNDR and 45dB SFDR over frequency and that the maximum DNL and INL are +0.93/-0.84 and +0.75/-1.02 LSB, respectively. Table I summarizes the ADC performance and compares this work against previous medium resolution ADCs

TABLE I: PERFORMANCE SUMMARY

References	VLSI'18 [5]	CICC'19 [6]	ISSCC'17 [7]	ISSCC'17 [3]	This Work
Technology (nm)	40	40	28	14	<b>14</b>
Supply (V)	1.2	1.1	0.9	0.95	<b>0.8</b>
Architecture	Two step SAR	2-3b SAR	1-2b SAR	Pipe-SAR	<b>Pipe-SAR</b>
Channels	1	1	2	1	<b>1</b>
Resolution (bits)	8	7	7	10	<b>8</b>
Sampling rate (GS/s)	1.1	0.9	2.4	1.5	<b>1.5</b>
ENOB @Nyquist	7.18	6.3	6.36	8	<b>6.58</b>
Area (mm <sup>2</sup> )	0.00165	0.014	0.0043	0.00158	<b>0.0013</b>
Power (mW)	4	2.6	5	6.9	<b>2.4</b>
FOM (fj/conver-step)	25	36.6	25.3	17.7	<b>16.7</b>

with GS/s sample rates. The pipelined-SAR architecture with the efficient OLS amplifier allows for 1.5GS/s operation at the lowest 0.8V supply and 2.4mW power consumption, while also achieving the best 16.7 fJ/conver-step FOM.

#### V. CONCLUSION

This paper presented a single channel 8-bit pipelined-SAR ADC that utilizes a novel low-overhead OLS settling technique in the dynamic residue amplifier. A low power design is realized by combining this technique with the use of parallel comparators in the two asynchronous pipeline stages to allow for 1.5GS/s operation with a low 0.8V supply voltage.

#### ACKNOWLEDGMENT

This work was supported in part by SRC TxACE Grant 2810.013 and NSF Grant 1930828.

#### REFERENCES

- [1] S. Palermo *et al.*, "Analog-to-digital converter-based serial links: an overview," in *IEEE Solid-State Circuits Magazine*, vol. 10, no. 3, pp. 35-47, Summer 2018.
- [2] S. Kiran *et al.*, "A 32 Gb/s ADC-based PAM-4 receiver with 2-bit/stage SAR ADC and partially-unrolled DFE," *IEEE CICC*, 2018.
- [3] L. Kull *et al.*, "28.5 A 10b 1.5GS/s pipelined-SAR ADC with background second-stage common-mode regulation and offset calibration in 14nm CMOS FinFET," *IEEE ISSCC*, 2017.
- [4] B. R. Gregoire *et al.*, "An over-60 dB true rail-to-rail performance using output level shifting and an opamp with only 30 dB loop gain," *IEEE JSSC*, vol. 43, no. 12, pp. 2620-2630, Dec. 2008.
- [5] H. Chen *et al.*, "A >3GHz ERBW 1.1GS/s 8B two-step SAR ADC with recursive-weight DAC," *IEEE VLSI Symp.*, 2018.
- [6] D. Li *et al.*, "A 7b 2.6mW 900MS/s nonbinary 2-then-3b/cycle SAR ADC with background offset calibration," *IEEE CICC*, 2019.
- [7] C. Chan *et al.*, "16.4 A 5mW 7b 2.4GS/s 1-then-2b/cycle SAR ADC with background offset calibration," *IEEE ISSCC*, 2017.

- [8] Zhu, Liao, Sumanta Basu, Robert A. Jarrow, and Martin T. Wells. "High-dimensional estimation, basis assets, and the adaptive multi-factor model." *Quarterly Journal of Finance* 10, no. 04 (2020): 2050017.